

^4He Films on Graphite Studied by Neutron Scattering*

H. J. Lauter

Institut Laue-Langevin, Grenoble, France

and

H. Godfrin

CNRS-CRBTB, Grenoble Cedex 9, France

and

P. Leiderer

University of Konstanz, Konstanz, Germany

The properties of ^4He films adsorbed on graphite have been studied by neutron scattering. In particular excitations of the commensurate phase of the monolayer are discussed. The first two adsorbed layers are solid and the next ones stay liquid. At the boundaries of the superfluid film excitations could be studied. Also the phonons, maxon and rotons of the film are investigated. An explanation of the lower density of the very thin films compared to bulk ^4He is given.

1. INTRODUCTION

The monolayer phase diagram of ^4He on graphite shows interesting features, of which the central one is the commensurate phase $(\sqrt{3} \times \sqrt{3})30^\circ$.¹ The existence of this phase could be proven by neutron diffraction.² But also the phonon gap at the zone center, the sign of loss of translational invariance, could be recently studied. From the phonon gap the curvature of the corrugation of the adsorption potential can be calculated. This has also been done in comparison with other adsorbates in the commensurate phase.³ A thicker ^4He film shows particular properties. The first two layers are solid on graphite but with very different densities.⁴ The subsequent layers are liquid. Thus the liquid film has two interfaces: The solid-liquid ^4He interface and the liquid-gas ^4He one. Concerning the liquid-solid boundary there the freezing-melting wave could be excited.⁵ Also, using

* Presented by H. J. Lauter.

inelastic neutron scattering, excitations with constant dispersion could be measured, which may play a role in the anomalous small Kapitza-resistance. At the gas-liquid boundary quantized capillary waves (ripples)⁶⁻⁹ can be excited. For the film itself it was measured that the superfluid onset temperature is shifted to lower temperatures with decreasing film thickness and a reduced superfluid fraction is detected.¹⁰⁻¹² This may be caused by a different excitation spectrum with respect to the bulk [e.g. Ref. 12]. In this report we will give some new information about the monolayer and excitations in a ⁴He film and at its boundaries.

2. EXPERIMENT

In contrast to previous neutron scattering experiments of ⁴He films,^{13,14} which were carried out using graphite powder as substrate, this time we used Papyex¹⁵ as substrate. Papyex has, besides a powder contribution, oriented graphite crystallites which show a 30° (FWHM) mosaic distribution with respect to the *c* axis. A densest first layer (which under consideration of the pressure of the second layer has a density of 0.115 atoms/Å²⁴) consisted of 312 cc (STP) ⁴He. The subsequent layers⁴ are taken to have densities of 0.95, 0.078, 0.078 atoms/Å² . . .

The inelastic neutron scattering experiments were performed partially for the monolayer experiments on triple axis spectrometers of which the set-up is explained in the later-mentioned references, whereas for the other experiments the time-of-flight spectrometer IN6¹⁶ at the ILL was taken with a chosen wavelength of 5.12 Å. The detectors of this spectrometer are located in an angular range of 11.9°-113°; this corresponds, for elastically scattered neutrons, to momentum transfers (*Q*) between 0.254 and 2.046 Å⁻¹. The energy resolution is only slightly dependent on *Q* and is about 0.055 meV for elastically scattered neutrons. The sample was mounted with the *c* axis perpendicular to the scattering plane. The data obtained from the sample cell including the graphite was used as background and subtracted from subsequent measurements with adsorbed ⁴He.

3. EXCITATIONS IN THE COMMENSURATE LAYER

The aim of neutron inelastic measurements is to determine the excitation spectrum of the different phases of adsorbates on graphite and in particular that of the commensurate phase. This has been done for many systems on graphite^{3,17} like krypton,¹⁸ methane,¹⁹ and nitrogen²⁰ but also quantum systems like hydrogen^{21,22} and helium²³ isotopes. These results have provided quantitative values against which the theoretical models of the adsorbate-substrate interaction potentials can be compared. But also

TABLE I

Parameters Characterizing the Phonon Density of States (DOS) for the In-Plane Modes of the Commensurate Phase of the Hydrogen Isotopes Adsorbed on Graphite

	H ₂	HD	D ₂
Zone center gap ²¹ (neutron scattering)	47.3 K	43.2 K	40.0 K
calculations from reference 24	39.1 K	—	31.2 K
calculations from reference 25	46.6 K	—	36.9 K
DOS width ²² (neutron scattering)	27.5 K	14.7 K	9.5 K
calculations from reference 25	42.1 K	—	14.8 K

the adsorbate-adsorbate interaction potential enters into these considerations and is very interesting because this potential is tested at the commensurate distance, which is in particular for the quantum systems very different from the natural one in the bulk phases. A review is given in Ref. 3, where also technical details are given.

The detailed knowledge of the adsorption potential is not only relevant for adsorbed monolayers, but is necessary to understand the gradual change of bulk properties that occur near an interface.

Here at first the comparison of experiment and theory of the hydrogens adsorbed on graphite is given in Table I. The measured zone center frequencies, which are a measure of the hydrogen-graphite corrugation, are in reasonable agreement with the calculations, but the width of the phonon density of states (DOS) are overestimated by theory. The interaction between the adsorbed molecules is weaker than expected and more theoretical work would be welcome. The mass dependence of the phonon spectrum cannot be explained with an isotopic effect only.

Only recently the zone center phonon gap of the commensurate phase of the He isotopes has been measured^{23,26} and are shown in Table II. The large neutron absorption cross section of ³He makes it extremely difficult

TABLE II

Parameters Characterizing the Phonon Density of States for the In-Plane Modes of the Commensurate Phase of the Helium Isotopes Adsorbed on Graphite

	³ He	⁴ He
Zone center gap ^{23,26} (neutron scattering)	11 K	11 K
calculations from reference 27	35 K	28 K
calculations from reference 24	16 K	16 K
DOS width ²³ (neutron scattering)	(?)38 K	—

to obtain reliable data. As discussed above, a corrected background has to be subtracted. ^4He , on the other hand, has a very small coherent neutron cross section which makes its measurement very difficult.

In conclusion the agreement between theoretical calculations for the commensurate phase and experimental values for the phonon gap is good for the hydrogens and to be improved for the heliums, but the interaction between adatoms is still overestimated. The measurements performed in the commensurate and also in the incommensurate phases³ allow the determination of elastic constants which are comparable with bulk systems under large positive and negative pressures. An adequate analysis of these data permits the determination of the interaction potential at distances that are hard to reach in 3-D matter. A precise knowledge of the graphite surface has an intrinsic interest that goes beyond the adsorbate monolayer regime.³

4. EXCITATIONS AT THE LIQUID-SOLID BOUNDARY

In previous experiments it was shown that excitations can be measured which are located at the liquid-solid ^4He interface. They have constant dispersion ("flat modes") indicating a localized character.^{13,14} This is shown in Fig. 1, where for a 6.4 ^4He layer film on Ne-coated graphite powder in addition to the bulk excitations these flat modes show up. Also in the case of Ne-coated graphite one solid ^4He layer is next to the Ne layers. The proof that these flat modes are localized at the liquid-solid ^4He boundary was given by the fact that they still persist in a sample cell completely filled with ^4He and that the intensity of these modes does not depend on the amount of adsorbed ^4He beyond a total coverage of four layers.¹⁴ Now we changed from the powder substrate to Papyex and the flat modes lost about 30% in intensity relative to the roton intensity at a same given coverage. Thus a more homogeneous substrate and/or the preferential orientation may reduce this signal.

The main origin of the flat modes was suggested to be an exchange of atoms between the second solid ^4He layer (pure graphite substrate) and the liquid ^4He . In order to test this idea we preplated the graphite with two layers of H_2 . The ^4He isotherm taken on the preplated graphite²⁸ shows that the density of the first ^4He layer of $0.072 \text{ atoms}/\text{\AA}^2$ is not high enough to be a solid, at least at the temperature of $T = 1.96 \text{ K}$. From Ref. 1 and 28 it can be deduced that about a density of $0.08 \text{ atoms}/\text{\AA}^2$ is needed to solidify an incommensurate monolayer of ^4He .

The comparison of a spectrum with and without preplating is shown in Fig. 2. The spectra have been taken at a constant angle, which corresponds to a $Q = 2.00 \text{ \AA}^{-1}$ on the elastic line. From Fig. 1 it is seen that this corresponds roughly to spectrum number 18 and this scan crosses the bulk

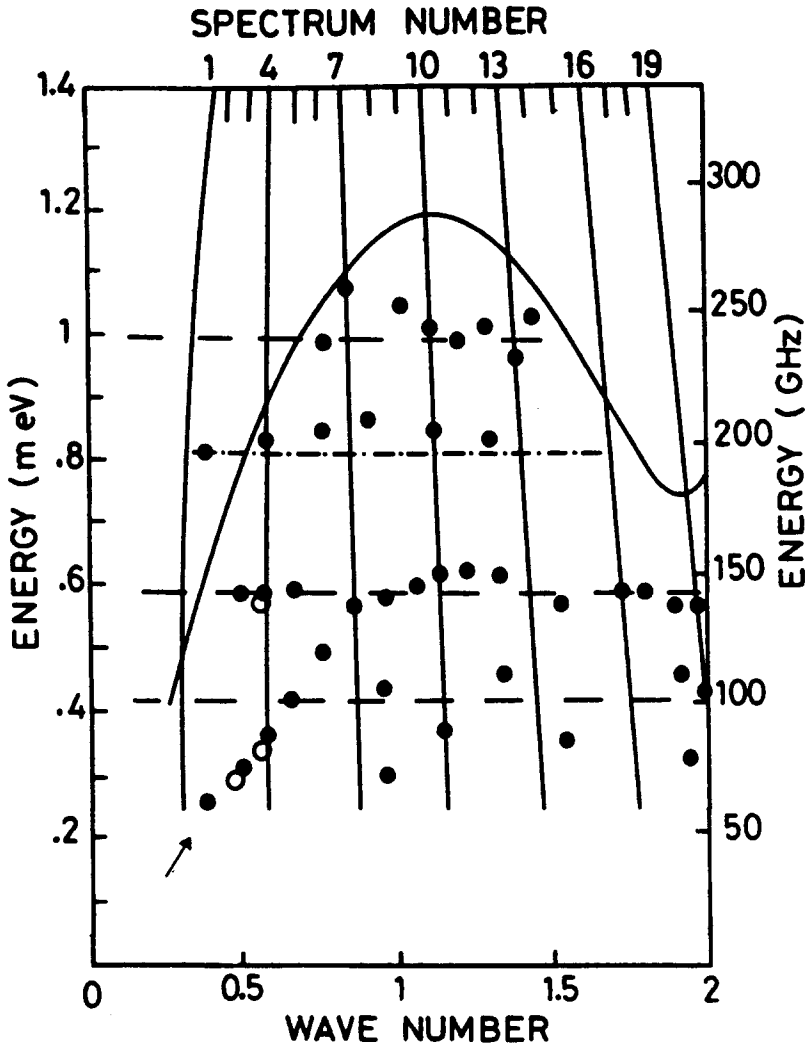


Fig. 1. Position of the signals in the energy-wavenumber plane from 6.4 ^4He layers on top of the Ne-coated graphite powder at $T = 0.5\text{ K}$.¹⁰ The spectra have been measured on a time-of-flight spectrometer, therefore the spectrum number indicates the path along which the spectra are taken with constant scattering angle. The solid line represents the bulk ^4He signals. The dashed-dotted line shows the peak position of the multiple scattering (diffraction of neutrons by the (002) graphite reflection and creation of a roton). Accidentally, this signal is superimposed on a localized mode which are otherwise marked by dashed lines. The arrow points to the first indication of the ripplon, which has been measured in 4.8 ^4He layers on Papyex (\circ).¹⁰ The intensity of this mode does not depend on the amount of adsorbed ^4He beyond a coverage of 4 layers.¹¹ In the present measurements we changed from the powder substrate to Papyex and the flat mode lost about 30% in intensity (normalized to the roton intensity). Thus a more homogeneous substrate and/or the preferential orientation may contribute to the decrease of the signal.

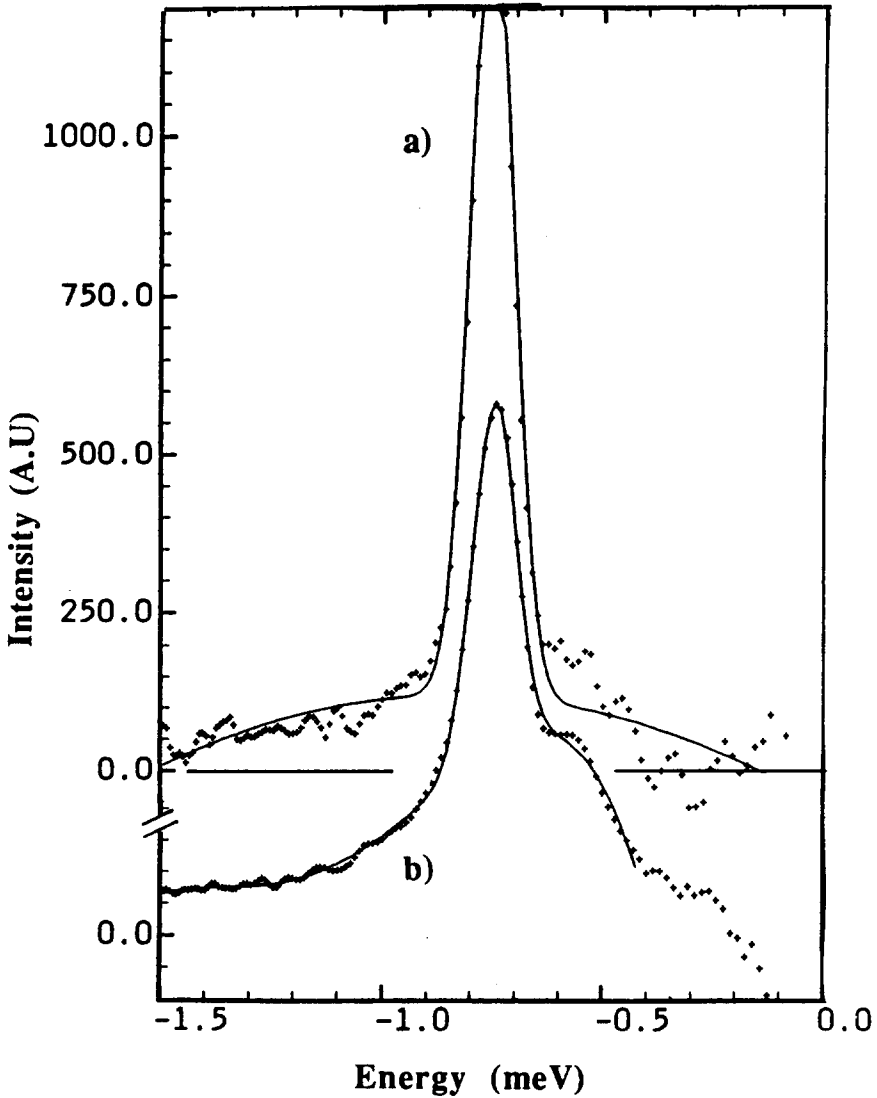


Fig. 2. Inelastic neutron scattering scans along the path of spectrum number 18 in Fig. 1 with an elastic $Q = 2.00 \text{ \AA}^{-1}$. In (a) (sample 1) the graphite was preplated by two layers of H_2 and subsequently 4.6 layers of ^4He are adsorbed. In (b) (sample 2) a pure graphite substrate was used with 5.06 adsorbed layers of ^4He in total. In both cases the roton shows up at an energy transfer of 0.755 meV. The flat mode intensity is at about 0.6 meV. The fit is a very rough one and focuses mainly on the roton. The temperature is 0.7 K. The ordinate is displaced by 250 units between 2(a) and 2(b). The energy scale is negative due to a convention on the IN6 spectrometer for the energy transfer. The absolute value is the energy transferred to the excitation.

dispersion at $Q = 1.92 \text{ \AA}^{-1}$ and at an energy of 0.755 meV. In both cases the roton excitation can be clearly seen. At a lower energy of 0.6 meV the intensity of a flat mode shows up. It is evident that this intensity decreases by a factor of two in the case of the preplated sample with respect to the intensity of the non preplated sample. This shows that the suppression of the solid ^4He layers decreases the intensity of the flat modes by an appreciable amount, so the conclusion is that the solid layers are involved in the local modes. These solid layers are present in most examples of Kapitza-resistance measurements and should be taken into consideration. The transmission of a phonon from a solid through an interface to liquid ^4He is considerably enhanced by the simultaneous excitation of a localized excitation and of a phonon (roton) in the superfluid, since the restrictions imposed by energy and momentum conservation are then relaxed.

Also the intensity of the bulk roton signal of the film on the different substrates can be compared. The intensity increases in the case of the preplated sample (called sample 1 with a filling of 4.6 layers) by a factor of 2.2 (same linewidth) with respect to the not preplated sample (sample 2 with a filling of 5.06 layers including the solid ones). This is mainly due to the replacement of the solid ^4He layers by liquid layers. A more careful consideration is given in the following: The filling was 5.06 layers of ^4He for sample 2. It will turn out (see Sec. 6) that 3.5 layers do not contribute to the intensity of phonons and rotons in this case: two solid layers and 1.5 inert layers, thus the signal intensity comes only from a layer of thickness of 1.56. An intensity gain of 2.2 was measured in switching to sample 1 (see Fig. 2; this factor is also confirmed at other Q s). This gives 3.43 layers which do contribute to the signal intensity for sample 1. The filling of sample 1 was 4.6 layers. Thus 1.2 layers do not contribute to the intensity of phonon and roton excitations (there are no solid layers). This is about the same number as on the pure graphite substrate, where 1.5 layers are inert (plus two solid layers makes the 3.5 layers). The information which can be taken from the phonon and roton signal intensity for the two different substrates is twofold. It firstly confirms that no solid ^4He layers are present in the case of the H_2 preplated sample and secondly it demonstrates that a liquid ^4He layer (1.2 to 1.5 layers) does not contribute to the intensity of the phonons and rotons in a ^4He film on different substrates.

5. EXCITATIONS AT THE LIQUID-GAS BOUNDARY

Quantized capillary waves (rippions) are the elementary excitations of a free liquid surface. Their existence at the bulk ^4He surface and in films has been predicted by theory and indirectly confirmed by experiment.^{6,29} At long wavelengths the ripplon dispersion relation is easily evaluated using

hydrodynamic relations for an incompressible fluid:

$$\omega^2 = (\alpha_0 / \rho_0) k^3 \quad (1)$$

where α_0 is the zero-temperature surface tension, ρ_0 the ^4He density at zero pressure, and k the wavevector. The temperature dependence of the surface tension ($\alpha(T)$) at very low temperatures can be deduced from the ripplon dispersion relation. Detailed measurements of $\alpha(T)$ ³⁰ revealed a much larger temperature dependence than expected from formula (1). Several modified dispersion curves have been proposed which differ mainly for wavevectors above 0.5 \AA^{-1} . The idea of a "surface roton", with a minimum at $\sim 2 \text{ K}$, was introduced by Reut and Fisher³¹ improving the agreement with the available thermodynamic data. Edwards *et al.*,^{6,30} taking into account the curvature dependence of α , were able to fit the experimental data on the excess surface entropy. Their model involves two parameters: a length $\delta = d(\ln \alpha_0) / dK$ where $K = (r_1^{-1} + r_2^{-1})$ is the curvature of the surface, and an area $a = d\delta / dK$. Several sets of parameters have been used [$a = 1.5 \text{ \AA}^2$, $\delta = 0$ ³⁰ and $a = +1.0 \text{ \AA}^2$, $\delta = -0.336 \text{ \AA}$ (Ref. 6)], the latter giving better agreement. Such a large variation in the parameters corresponds to very different ripplon dispersion curves at wavevectors $\sim 1 \text{ \AA}^{-1}$, with a common trend indicating the presence of a downward curvature. Little direct experimental evidence was available,¹³ however, on the ripplon dispersion curve at these wavevectors. Such a study requires a microscopic probe like inelastic neutron scattering (INS), but due to the low neutron cross section of ^4He the measurement has to be performed on samples with a large surface to volume ratio. The success of a neutron total reflection experiment is, however, not yet excluded.³²

A first outline of the experiment of which some results are depicted in Fig. 3 was already given in Refs. 33 and 34. In Fig. 3 the different stages of gray indicate the behaviour of the intensity as a function of energy and momentum transfer. It is clearly seen in Fig. 3(a) that besides the intensity on the phonon-roton curve there is intensity on an energetically lower-lying branch. Evidence of the existence of this branch has been given previously on measurements.^{13,14} This branch coincides with the calculated dispersion of the ripplon using the parameter set in Ref. 6. The agreement is very good: it seems to be even up to 1.5 \AA^{-1} . At still higher Q the roton intensity combined with the one of the flat modes becomes too high to distinguish the ripplon signal. This good agreement allows us to say that the temperature dependence of the surface tension is really based on an experimentally verified dispersion relation. It still remains to prove the modified parameter set of Ref. 6 by theory.

In Fig. 3(b) the result of the completely filled sample cell is shown. In the region where the ripplon should show up, the scale of the greys is the

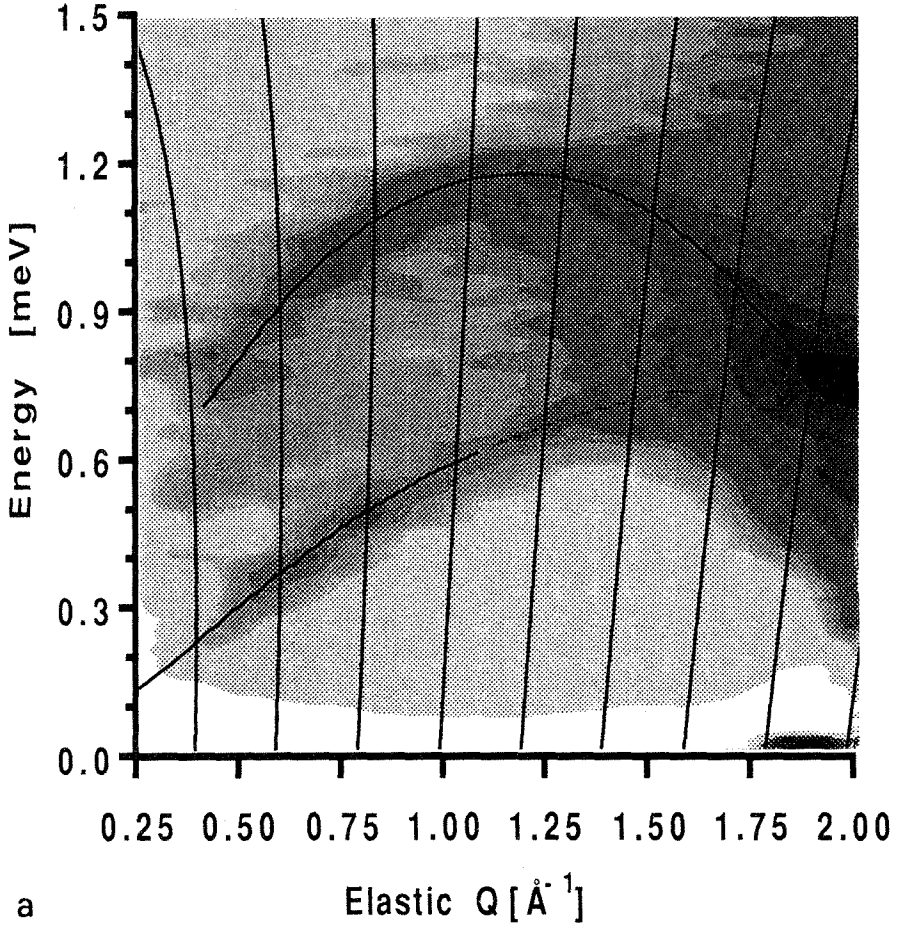


Fig. 3. Intensity on the phonon-rotor curve and on the ripplon curve in the energy- Q plane. The intensity is given by the different grey stages. It increases from white to black. The black lines represent the phonon-maxon-rotor curve³⁷ and the ripplon dispersion.⁶ Figure 3(a) shows the signal from 5.06 adsorbed layers on graphite and Fig. 3(b) the signal from the sample cell completely filled with ^4He (background is subtracted, which is the intensity from the sample without helium).

same as in Fig. 3(a). Only near the phonon-rotor intensity and the flat bar of the multiple scattering^{13,14} the attribution of the different greys to intensity has been modified. Thus the figure shows that no signal of the ripplon intensity is visible in (Fig. 3(b)) the filled cell, although below 0.7 \AA^{-1} it would have been distinguishable from the overwhelming quasi bulk phonon

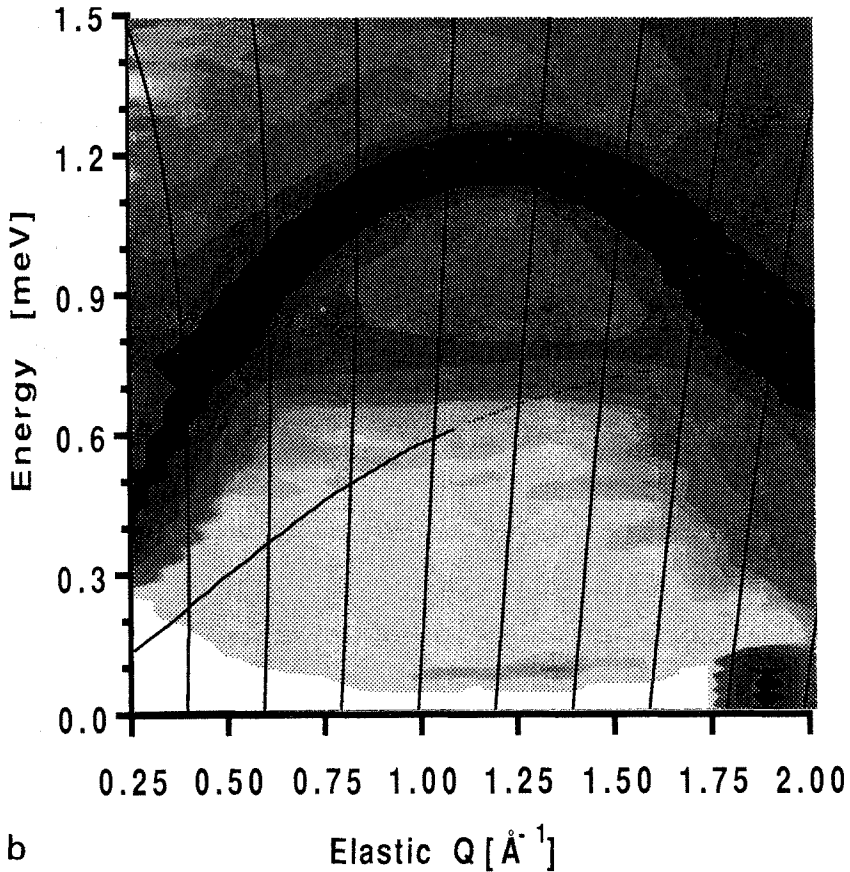


Fig. 3. Continued.

roton intensity. This disappearance proves that the ripplon signal is really bound to the gas-liquid interface.

A more detailed description of the ripplon dispersion is seen in Fig. 4. The measured dispersion agrees indeed very well with the calculation in Ref. 6 up to $Q = 1 \text{ \AA}^{-1}$. But between 0.6 and 1 \AA^{-1} a small but measurable increasing slope of the dispersion curve with decreasing film thickness has been detected indicating a stiffening of this mode may be due to a variation of the surface tension α with the film thickness. The behavior at higher Q let us assume a minimum in the dispersion curve. However, this comes about due to crossing the flat mode at 0.6 meV and each negative slope is due to the fit-routine, which clamps with increasing Q to the higher intensity

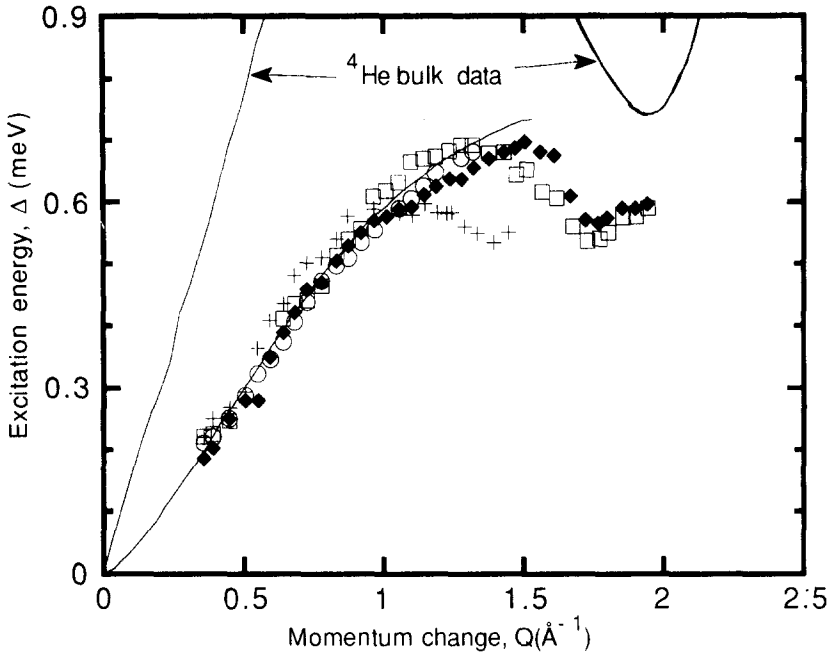


Fig. 4. The ripplon dispersion for various coverages. The total He layer thickness is (○), 4.16 layers (◆), 3.85 layers (□) and 3.54 layers (+). The ripplon dispersion curve is shown as full line.⁶

of the flat mode. An interaction between the ripplon and the flat mode in a thin film is not excluded¹⁴ but needs further consideration. We can confirm a positive slope of the dispersion curve in agreement with Ref. 6 up to 1.3 \AA^{-1} for certain coverages. At higher Q the ripplon intensity gets lost.

The intensity of the ripplon is plotted in Fig. 5 as a function of Q for the different coverages. The ripplon is most intense at low Q losing its intensity rapidly up to 0.6 \AA^{-1} . At higher Q again the interference with the flat modes makes correct data analysis impossible, in particular to the half automatic fit-routine. A further data analysis of the experiments of the helium film on a H_2 preplated graphite surface will give more information.

From preferential Q , which are free from the flat mode intensity, ripplon intensities can be taken by careful fitting as a function of coverage. For a Q of 1.2 \AA^{-1} this has been done and is shown in Fig. 6. The ripplon intensity seems to saturate beyond a coverage of five layers. This is in agreement with the picture of a surface wave, whose intensity does not depend on the amount of bulk liquid below the surface. On the other hand the ripplon intensity disappears below three layers. Since two layers are solid, this is in agreement with a penetration depth of about an atomic layer.^{6,8} However,

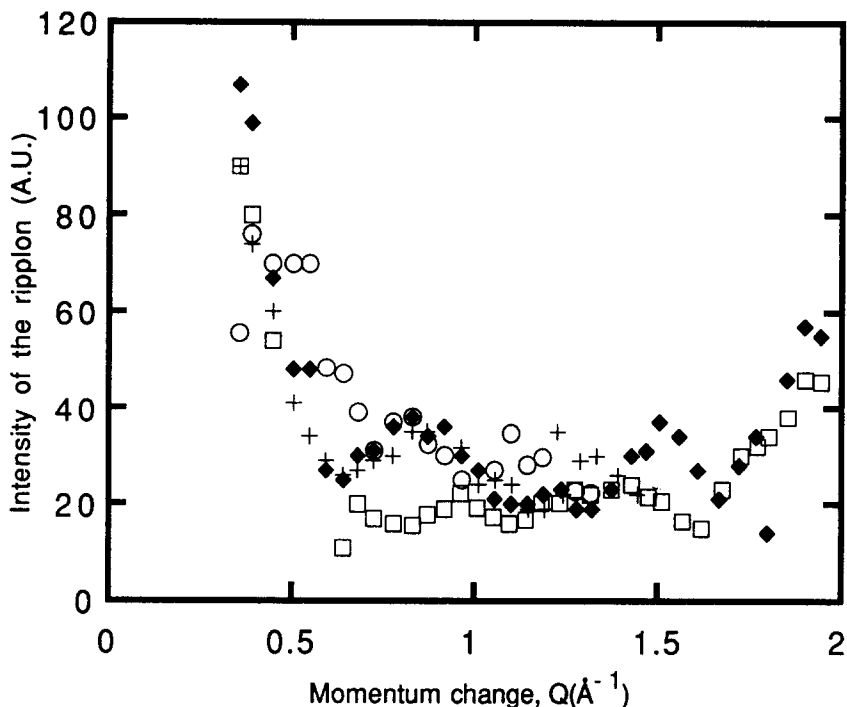


Fig. 5. The intensity of the ripplon as a function of Q for various coverages. The total ${}^4\text{He}$ layer thickness is 5.06 layers (○), 4.16 layers (◆), 3.85 layers (□) and 3.54 layers (+).

this intensity disappears definitely at a lower coverage than the phonon-ripplon intensity. This phenomenon is not yet understood.

Other modes are predicted for a thin film between the ripplon and the continuum (the phonon-rotor dispersion curve)^{7,8,35} but up to now no other modes could be detected.

6. PHONONS AND ROTONS IN A ${}^4\text{He}$ -FILM

A long-outstanding question is how the dispersion curve of bulk liquid ${}^4\text{He}$ is changed if the ${}^4\text{He}$ is confined in a film. A very simple approach was given in Ref. 12 where a change in the static structure factor was calculated in going from three-dimensional ${}^4\text{He}$ to two-dimensional ${}^4\text{He}$. This shift results in a lowering of the roton minimum and a shift toward lower energies. Our scans hardly approached the roton minimum in Q and on the other hand this theory was not made for the phonons and maxons. Thus another theory was considered.^{7,35} Here a clear increase of the energy in the maxon

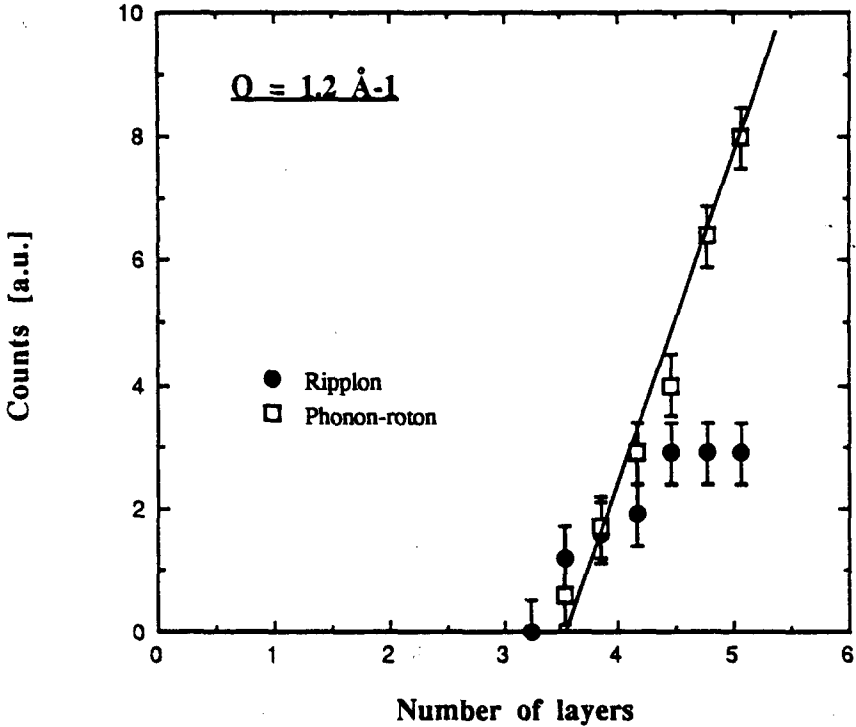


Fig. 6. Intensities of the phonon (○) and ripplon (●) as a function of coverage at $T = 0.7$ K.

region was predicted due to the higher density regions of the liquid layers near the solid. However, our fits to the experimental data, exhibited in Fig. 7, show that a lowering of the dispersion curve takes place in the maxon region if the film thickness is reduced. The lowering of the dispersion curve is continued towards the roton minimum. However, the roton minimum was not covered by these scans. But in comparable experiments of a ^4He film in Vycor glass a shift of the roton minimum energy towards higher energies was detected in addition to the shift of the maxon energy towards lower energies already seen on a graphite substrate. This is a clear sign of a lower density in the film. These reduced densities can be estimated from an extrapolation of the curve of the maxon energy as a function of density depicted in Fig. 8. The values of the derived densities are 0.1402 g cm^3 for 3.85 layers, 0.1413 g cm^3 for 4.16 layers and 0.1429 g cm^3 for 5.06 layers.

The question is now how a ^4He film can have a lower density than bulk helium. Recently the density profile of ^4He have been calculated by different theories.^{7,35,36} In particular the densities calculated by Ref. 36 show

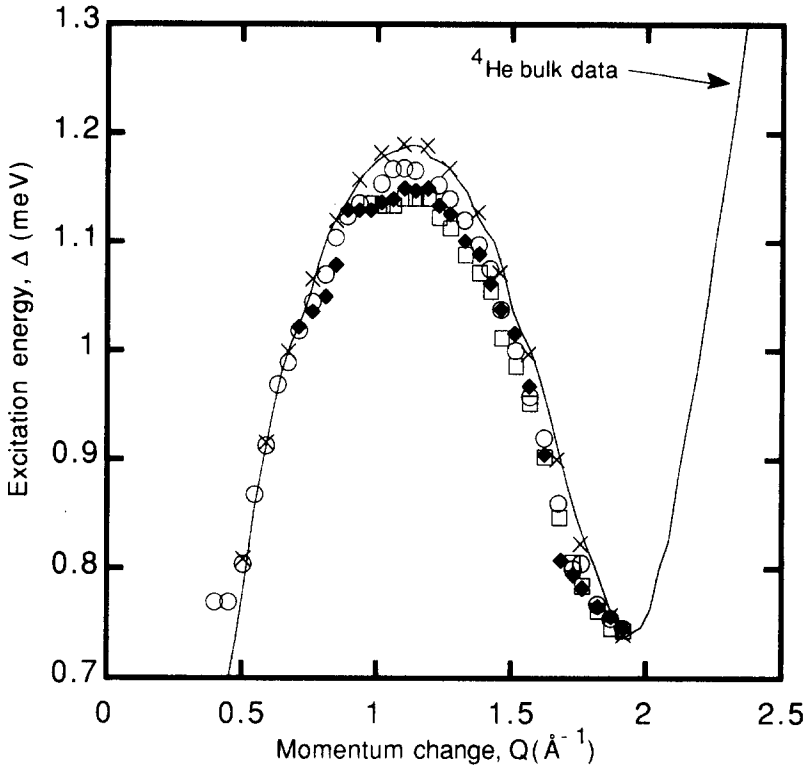


Fig. 7. Variation of the dispersion relation of the phonons and rotons as a function of film thickness at a temperature of 0.7 K. The total ${}^4\text{He}$ layer thickness is 5.06 layers (O), 4.16 layers (\blacklozenge) and 3.85 layers (\square). (\times) marks data from the cell completely filled with He.

a very good agreement of the densities of the first two layers with the densities derived from diffraction experiments.⁴ This profile is shown in Fig. 9 for various thicknesses of the ${}^4\text{He}$ film. All these thicknesses were studied by neutron scattering; here we select the three already mentioned. Phonons and rotons cannot be excited over the whole film thickness. As already mentioned the first two layers are solid and thus no excitations can be created (in our energy-momentum range), as well as in the 1.5 liquid layers adjacent to the substrate (inert layers; see later discussion of Fig. 6). It is clearly seen in Fig. 9 that the average density of the film beyond 11.1 Å (the nominal thickness of 3.5 layers) is lower than the bulk density of 0.0218 atoms/Å³, thus the excitations created in this part of the film reflect this lower density.

In a further step the density derived from the scattering data in Fig. 8 can be taken for each of the three coverages. These densities belong to the

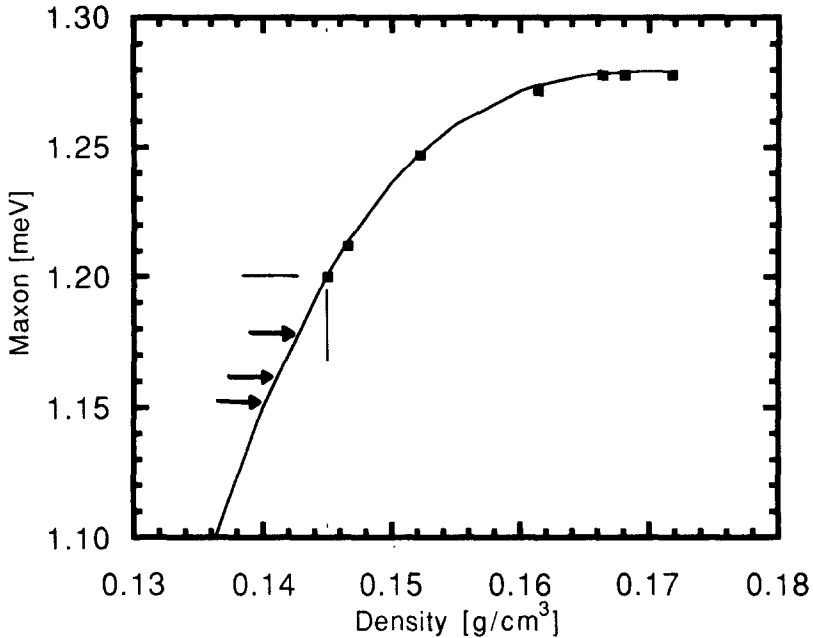


Fig. 8. Energy of the maxon as a function of density. The arrows below the energy of 1.2 meV, the bulk value under saturated vapor pressure (the coordination of which are marked by straight lines), are at values of the maxon energy which are derived from Fig. 7 and point for the three different film thicknesses to the deduced average densities.

film beyond the 11.1-Å-thick inert part. Now the densities derived from the calculation and from the experiment can be compared. First the integral over the calculated profile can be taken also beyond 11.1 Å, this gives the areal density of this special part of the film. Next the areal densities of this calculation and the ones from the average density of the experiment (from Fig. 8) are set equal. By this procedure the second boundary value for the experimental densities is deduced. The first boundary value is still 11.1 Å. These second boundary values are marked by arrows for the different films. They represent an average thickness of the film belonging to the average measured density. Thus excitations can be created between 11.1 Å and the second boundary. The second boundaries are roughly situated at the point where the film has decreased to half density of the density profile near the last drop to the gas phase. This is what is expected, so there is agreement between experiment and theory.

It should be mentioned that our data from the cell completely filled with ^4He (not corrected for a little instrument resolution effect) agree with the bulk dispersion curve.³⁷

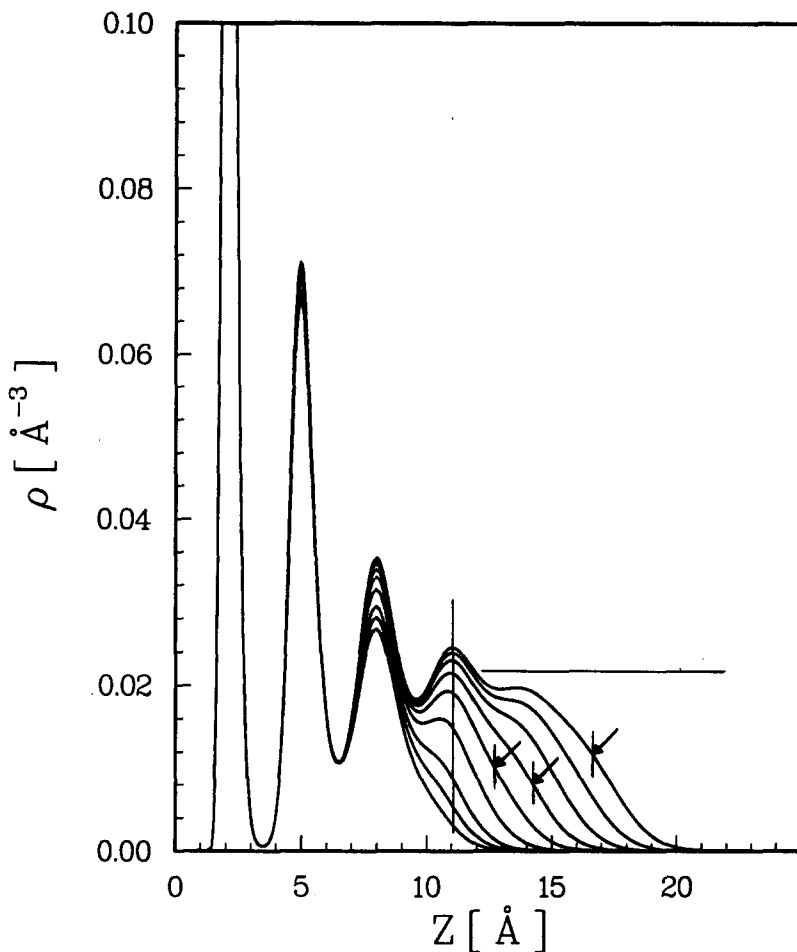


Fig. 9. Density profiles of ${}^4\text{He}$ films.³⁶ The curves are for nominal densities (see chapter experiment) of 2.96, 3.09, 3.24, 3.54, 3.85, 4.16, 4.46, 4.76, and 5.06 layers, among which figure the densities of Fig. 7. The 3.5 inert layer thickness is marked by a vertical line at 11.1 Å. The bulk density is marked by a horizontal line. For further discussion see text.

The intensity of the phonons and rotons is plotted in Fig. 10. A calibration to the bulk data was done for all film thicknesses at a Q of 1.92 \AA^{-1} . The data taken with the cell completely filled with ${}^4\text{He}$ show toward lower Q a small deviation to lower intensities with respect to the bulk data. We do not know yet whether this is significant. Important deviations appear, however, for the ${}^4\text{He}$ films. The thick film (5.06 layers) loses much intensity below a Q of 0.7 \AA^{-1} . This Q corresponds just to the liquid film thickness. Thus the loss of the third dimension reduces the

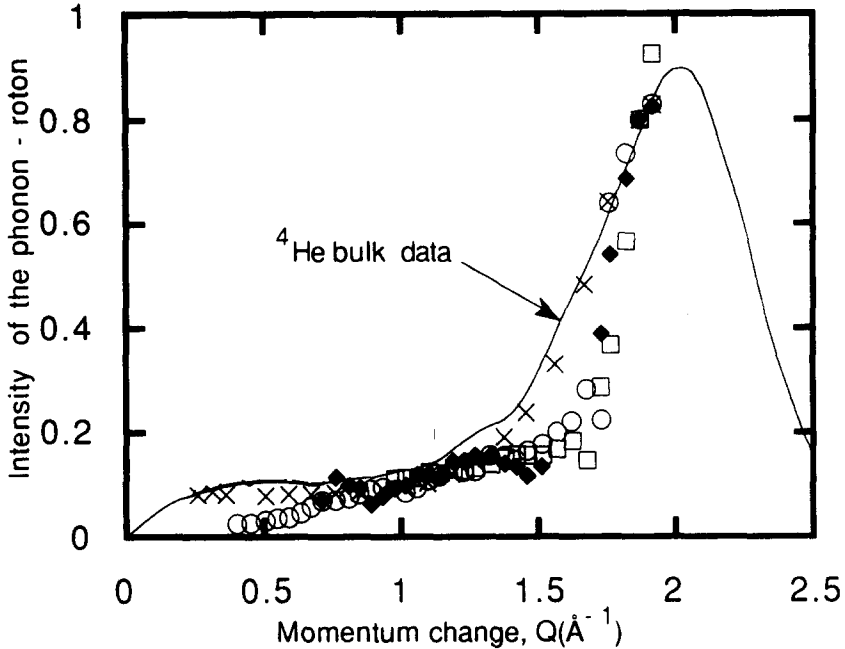


Fig. 10. Intensity of the phonons and rotons as a function of Q at a temperature of 0.7 K. The total ^4He layer thickness is 5.06 layers (\circ), 4.16 layers (\blacklozenge) and 3.85 layers (\square). (\times) marks data from the cell completely filled with helium. The intensities of the different coverages are calibrated to 0.8, the value of the bulk data at 1.92 \AA^{-1} .

intensity of the phonon. The thinner films show at low Q no more intensity. Thus a loss in intensity is detected if the film thickness correlates with the momentum transfer of the excitation and the intensity disappears even at still lower Q .

Another remarkable feature in figure 10 is the loss of intensity with respect to the bulk data around 1.7 \AA^{-1} . We can only suggest that this effect may again result from the reduced dimensionality, perhaps in connection with the negative group velocity of the excitations in this region.

The behavior of the intensity of the phonon was already shown in Fig. 6 against the film thickness for a Q of 1.2 \AA^{-1} . The intensity extrapolates to zero intensity at a total coverage of 3.5 layers. This coincides with measurements in Ref. 38, where a loss of superfluidity is detected at about 3 adsorbed layers. The question remains whether superfluidity disappears at 3.5 layers, where the signal of the phonon-roton disappears or at 3 layers where the ripplon disappears. The ripplon of a film between 3 and 3.5 layers shows no sign of additional damping, which is a necessary sign of the loss of superfluidity. So it is likely that the film is superfluid down to a coverage

of 3 layers, and that the role of the "superfluid phonon" is taken over by the ripplon.¹¹ The consequences of whether, due to this role, the ripplon should show a minimum like the roton are beyond this discussion.

CONCLUSION

In summary it turns out that the excitations in a commensurate monolayer film of helium give important results concerning the interaction potentials between the adsorbate-substrate but also between the adsorbate-adsorbate. The liquid helium film exhibits a lot of interesting features in the excitation spectrum. The excitation spectrum of the bulk phonon-roton curve is modified in a helium film as well as the dependence of the intensity on the momentum transfer. There are in addition excitations which have no dispersion (localized modes) at the solid-helium-liquid-helium interface. Finally the dispersion curve of the ripplon at the gas-liquid boundary could be measured for the first time to relatively high momentum transfers.

ACKNOWLEDGMENTS

It is a pleasure to thank J. Treiner for many stimulating discussions and for transmitting his calculations prior to publication. This work has been partially supported by the German Federal Ministry of Research and Technique (BMFT).

REFERENCES

1. R. E. Ecke and J. G. Dash, *Phys. Rev. B* **28**, 3738 (1983).
2. H. J. Lauter, H. Wiechert and R. Feile, in *Ordering in Two Dimensions*, S. K. Sinha ed. (North-Holland 1980), p 291; for ³He: M. Nielsen, J. P. McTague and W. Ellenson, *J. Physique*, Colloque C4, **38**, 10 (1977); H. J. Lauter, H. Godfrin, V. L. P. Frank and H. P. Schildberg, *Physica* **156 & 157**, 597 (1990).
3. V. L. P. Frank, H. J. Lauter, H. Godfrin and P. Leiderer, in *Excitations in Two-Dimensional and Three-Dimensional Quantum Fluids*, A. F. G. Wyatt and H. J. Lauter, eds. (Plenum Press, New York, 1991), Series B: Physics Vol. 257 p.489.
4. H. J. Lauter, H. P. Schildberg, H. Godfrin, H. Wiechert and R. Haensel, *Can. J. Phys.* **65**, 1435 (1987).
5. K. O. Keshishev, A. Ya. Parshin, and A. B. Babkin, *Sov. Phys.-JETP* **53**, 362 (1981).
6. D. O. Edwards and W. F. Saam, *Progress in Low Temperature Physics*, D. F. Brewer, (North-Holland, Amsterdam, 1978), Vol. 7A, p. 283.
7. E. Krotscheck, S. Stringari and J. Treiner, *Phys. Rev. B* **35**, 4754 (1987); J. L. Epstein and E. Krotscheck, *Phys. Rev. B* **37**, 1666 (1988).
8. G. Ji and M. Wortis, *Phys. Rev. B* **34**, 7704 (1986).
9. W. F. Vinen, *Springer Series in Solid State Science*, K. Ohbayashi & M. Watabe, eds. (Springer, Berlin, 1989), Vol. 79, p. 189.
10. M. Chester, *Comments Solid State Phys.* **10**, 91 (1981).
11. W. F. Saam and M. W. Cole, *Phys. Rev. B* **11**, 1086 (1975).
12. W. Götze and M. Lücke, *J. Low Temp. Phys.* **25**, 671 (1976).
13. H. J. Lauter, H. Godfrin and H. Wiechert, *Phonon Physics*, J. Kollar *et al.*, eds., (World Scientific, Singapore, 1985, p. 842).

14. H. J. Lauter, V. L. P. Frank, H. Godfrin and P. Leiderer, *Springer Series in Solid State Science* K. Ohbayashi & M. Watabe, eds (1989) (Springer, Berlin, 1989), Vol. 79, p. 99.
15. Papyex is a trademark of Carbone Lorraine, France.
16. *Guide to Neutron Research Facilities* from the ILL.
17. H. J. Lauter, H. Godfrin, V. L. P. Frank and P. Leiderer, in *Phase Transitions in Surface Films 2*, H. Taub, G. Torzo, H. J. Lauter and S. C. Fain, eds., NATO ASI Series, series B: Physics Vol. 267, p. 135 (1990).
18. V. L. P. Frank, H. J. Lauter, and H. Taub, unpublished data.
19. T. Moeller, H. J. Lauter, V. L. P. Frank and P. Leiderer, in *Phonons 89*, S. Hunklinger, W. Ludwig & G. Weiss, eds (World Scientific, Singapore, 1990), p. 919.
20. F. Y. Hansen, V. L. P. Frank, H. Taub, L. W. Bruch, H. J. Lauter, and J. R. Dennison, *Phys. Rev. Lett.* **64**, 764 (1990).
21. V. L. P. Frank, H. J. Lauter, and P. Leiderer, *Phys. Rev. Lett.* **61**, 436 (1988).
22. H. J. Lauter, V. L. P. Frank, P. Leiderer, and H. Wiechert, *Physica B* **156** & **157**, 280 (1989).
23. V. L. P. Frank, H. J. Lauter, H. Godfrin, and P. Leiderer, *Phonons 89*, S. Hunklinger, W. Ludwig, & G. Weiss, eds. (World Scientific, Singapore, 1990) p. 1001. The value for the gap quoted in this work was 13 K. This corresponds to the peak value of the spectrum. Taking into account the convolution with the resolution function of the spectrometer shifts it down to 11 K.
24. J. M. Gottlieb and L. W. Bruch, *Phys. Rev. B* **40**, 148 (1989); J. M. Gottlieb and L. W. Bruch, *Phys. Rev. B* **41**, 7195 (1990).
25. A. D. Novaco, *Phys. Rev. Lett.* **60**, 2058 (1988).
26. V. L. P. Frank, H. J. Lauter, H. Godfrin, and P. Leiderer, preliminary data obtained in a test measurement. The value of 11 K quoted for the gap takes into account the spectrometer resolution.
27. X.-Z. Ni and L. W. Bruch, *Phys. Rev. B* **33**, 4584 (1986); L. W. Bruch, in *Phase Transitions in Surface Films 2*, H. Taub, G. Torzo, H. J. Lauter, and S. C. Fain, eds., NATO ASI Series, series B: Physics Bol. 267, p. 67 (1990).
28. Measurements of T. Moller at the ILL in comparison with experiments in Ref. 1 and Motteler Ph.D. thesis, Univ. of Washington, 1985.
29. W. F. Vinen, *Springer Ser. in Sol. St. Sci.*, K. Ohbayashi & M. Watabe, eds. (Springer, Berlin, 1989) Vol. 79, p. 189.
30. D. O. Edwards, J. R. Eckardt, and F. M. Gasparini, *Phys. Rev. A* **9**, 2070 (1974).
31. S. Reut S and I. Z. Fisher, *Sov. Phys.-JETP* **33**, 981 (1971).
32. W. F. Saam, *Phys. Rev. A* **8**, 1048 (1973).
33. H. Godfrin, V. L. P. Frank, H. J. Lauter and P. Leiderer, in *Phonons 89*, S. Hunklinger, W. Ludwig and G. Weiss, eds (World Scientific, Singapore, 1989), p. 904.
34. H. J. Lauter, H. Godfrin, V. L. P. Frank, and P. Leiderer, in *Excitations in Two-Dimensional and Three-Dimensional Quantum Fluids*, A. F. G. Wyatt and H. J. Lauter, eds. Plenum Press, Series B: Physics Vol. 257, (1991) p. 419.
35. E. Krotscheck and C. J. Tymczak, in *Excitations in Two-Dimensional and Three-Dimensional Quantum Fluids*, A. F. G. Wyatt and H. J. Lauter, eds., Plenum Press, Series B: Physics Vol. 257 (1991) p. 257.
36. J. Treiner, private communication.
37. A. D. B. Woods and R. A. Cowley, *Rep. Prog. Phys.* **36**, 1135 (1972).
38. M. H. W. Chan, private communication.